

ESD RECORD COPY

RETURN TO
SCIENTIFIC & TECHNICAL INFORMATION DIVISION
(ESTI), BUILDING 1211

SIMPLE ANALYTICAL FUNCTIONS WHICH PROVIDE
MAGNITUDES OF RANGE AND ANGLE ERRORS FOR
PROPAGATION IN AN EXPONENTIAL ATMOSPHERE

Lyall G. Rowlandson

19 January 1968

ESD ACCESSION LIST

ESTI Call No. 62787

Copy No. 1 of 2 cys.

AEROSPACE INSTRUMENTATION PROGRAM OFFICE
ELECTRONIC SYSTEMS DIVISION
AIR FORCE SYSTEMS COMMAND
UNITED STATES AIR FORCE
L. G. Hanscom Field, Bedford, Massachusetts

This document has been
approved for public release and
sale; its distribution is
unlimited.

(Prepared under Contract No. F19628-68-C-0209 by Syracuse University
Research Corporation, Merrill Lane, University Heights, Syracuse, New York.)



AD676964

LEGAL NOTICE

When U. S. Government drawings, specifications or other data are used for any purpose other than a definitely related government procurement operation, the government thereby incurs no responsibility nor any obligation whatsoever; and the fact that the government may have formulated, furnished, or in any way supplied the said drawings, specifications, or other data is not to be regarded by implication or otherwise as in any manner licensing the holder or any other person or conveying any rights or permission to manufacture, use, or sell any patented invention that may in any way be related thereto.

OTHER NOTICES

Do not return this copy. Retain or destroy.



SIMPLE ANALYTICAL FUNCTIONS WHICH PROVIDE
MAGNITUDES OF RANGE AND ANGLE ERRORS FOR
PROPAGATION IN AN EXPONENTIAL ATMOSPHERE

LyaII G . Rowlandson

19 January 1968

AEROSPACE INSTRUMENTATION PROGRAM OFFICE
ELECTRONIC SYSTEMS DIVISION
AIR FORCE SYSTEMS COMMAND
UNITED STATES AIR FORCE
L. G. Hanscom Field, Bedford, Massachusetts

This document has been
approved for public release and
sale; its distribution is
unlimited.

(Prepared under Contract No. F19628-68-C-0209 by Syracuse University
Research Corporation, Merrill Lane, University Heights, Syracuse, New York.)

FOREWORD

This report is prepared for the

Aerospace Instrumentation Program Office
Electronics Systems Division
Air Force Systems Command of the United States Air Force
L. G. Hanscom Field
Bedford, Massachusetts

Air Force Program Monitor - Lt. K. Troup, ESD/ESSIE

Project Number 6684, Task 6684.05

covering research over the period

1968 February 1 to 1968 September 1

Prepared under Contract No. F19628-68-C-0209 by

Syracuse University Research Corporation
Merrill Lane, University Heights
Syracuse, New York

This report was reviewed and approved by

James Shunk, Captain, USAF
Program Manager for ESD/ESSIE/6684.

ABSTRACT

Range and angle errors produced by radio ray refraction are shown to be calculable from closed form exponential expressions. These expressions are developed from the error function equations derived by Freeman and apply to propagation in an exponential model atmosphere. The exponential expressions are further empirically modified to provide error data using the directly available radar tracking parameters, that is, apparent elevation angle and range. It is further shown that the elevation and doppler error angles may be derived from the exponential expressions.

TABLE OF CONTENTS

	<u>Page</u>
Foreword	ii
Abstract	iii
1. Introduction	1
2. The Simplification and Modification of the Equations Derived from Slant-Path Integration	3
3. A Correction at Small Elevation Angles	6
4. The Effect of Reduced Ranges	9
5. The Sensitivity of Calculated Magnitudes With Respect to Changes in the Exponential Model Profile	13
6. A Method to Determine the Elevation Angle Error	16
7. An Approximate Solution for the Doppler Velocity Error Angle	21
8. Some Final Comments	26
References	27

LIST OF ILLUSTRATIONS

<u>Figure</u>		<u>Page</u>
1	Ray Geometry	4
2	Range Error Versus Initial Elevation Angle - Long Range Case (600 km)	8
3	Range Error Versus Initial Elevation Angle - Variable Range Case	11
4	Total Path Bending Versus Initial Elevation Angle - Variable Range Case	12
5	Range Error Versus Initial Elevation Angle - Effect of Large Change in Refractivity Profile	14
6	Total Path Bending Versus Initial Elevation Angle - Effect of Large Change in Refractivity Profile	15
7	Ray Geometry Used to Calculate the Elevation Angle Error	17
8	Elevation Angle Error Versus Initial Elevation Angle - Long Range Case (600 km)	19
9	Elevation Angle Error Versus Initial Elevation Angle - Medium Range Case (200 km)	20
10	Doppler Error Angle Geometry	23
11	Doppler Velocity Error Angle Versus Initial Elevation Angle - Long Range Case (600 km)	25

1. INTRODUCTION

The correction for range and angle errors during real-time radar or optical tracking operations generally requires the piecewise solution of Snell's ray-tracing equations using digital computers. Two approaches can be taken.

In the first case, the atmosphere is frozen in time and space and the various errors are calculated based upon a description of the environment obtained from direct measurements with instrumentation. During the actual tracking operation the measured ranges and angles are then corrected by extracting the error data from storage. This procedure may be impractical due to the assumption of a frozen atmosphere, instrumentation limitations, the availability of sufficient computer storage and the data access time.

In the second case, the requirement to measure, assimilate, and process environmental data is removed by the tacit assumption that the environment can be defined by a simple analytical model, for example, an exponential decrease of the index of refraction with height. This definition may be quite acceptable; in which case, the propagation errors can be more readily determined in real-time. Even in this simplified situation the computation time required to calculate the errors from the ray tracing equations is not insignificant, if a high calculation accuracy is to be maintained.

It is therefore advantageous to obtain simple, closed form equations to calculate tracking errors in real-time. This approach eliminates the requirement for ray-tracing calculations, storage of error data and avoids limitations in the access time to retrieve stored data.

Since the index of refraction tends to decrease exponentially with height, the exponential model has gained wide application. Studies in its use have led to the well-known CRPL surface corrected model which attempts to adapt itself to locally varying conditions.^{1,2}

Using an exponential model Thayer and Freeman showed that errors produced by refraction could be represented by error function expressions.^{3,4,5}

This paper shows how these expressions may be replaced by exponential functions and empirically adjusted for use at low elevation angles and all practical ranges. Finally, these exponential expressions are used to derive equations to calculate elevation and doppler error angles.

In the development of these expressions the tracking parameters, where introduced, are in terms of the apparent elevation angle and range of the target since these variables are directly available from tracking systems.

2. THE SIMPLIFICATION AND MODIFICATION OF THE EQUATIONS DERIVED FROM SLANT-PATH INTEGRATION

The solution of the range error and total path bending integrals was carried out in Freeman's development by integration along the slant-path, R_0 , to the target.^{4,5} (Reference Figure 1.) This approach is justified by the fact that the range error due to the decrease in propagation velocity is much larger than the increased geometrical range along the curved path R . It is apparent that the height to any point, P , on path R_0 can be related to the geometric distance, S , and the true elevation angle, β_0

Using an exponential refractivity model,

$$N = N_s \exp(-ch) \quad (1)$$

where N_s = the station refractivity (N units)
 c = the decay constant (km^{-1})

Freeman then showed that the range error and total path bending integrals could be solved to give

$$\Delta R = 10^{-8} \int_0^S N \, ds = \frac{(\pi)^{\frac{1}{2}} g \exp(g^2) N_s}{10^8 c \sin \beta_0} \left[\operatorname{erf} \left(R_0 \cos \beta_0 \left(\frac{c}{2 r_0} \right)^{\frac{1}{2}} + g \right) - \operatorname{erf}(g) \right] \quad (2)$$

$$\tau = -10^{-8} \int_{\theta_0, N_0}^{\theta_r, N_r} \cos \theta \, dN = - \frac{(\pi)^{\frac{1}{2}} g \exp(g^2) N_s}{10^8 \tan \beta_0} \left[\operatorname{erf} \left(R_0 \cos \beta_0 \left(\frac{c}{2 r_0} \right)^{\frac{1}{2}} + g \right) - \operatorname{erf}(g) \right] \quad (3)$$

where $g = \left(\frac{c r_0}{2} \right)^{\frac{1}{2}} \tan \beta_0$
 r_0 = the earth radius (km)

Again, the range error used throughout this discussion is defined to be the difference between the radio path length along R (propagation dependent) and the geometric slant range, R_0 .

The first step in the modification of these equations is to note⁶ that

$$\frac{1}{x + (x^2 + 2)^{\frac{1}{2}}} \leq \exp(x^2) \int_x^{\infty} \exp(-t^2) \, dt \leq \frac{1}{x + (x^2 + 4/\pi)^{\frac{1}{2}}} \quad (4)$$

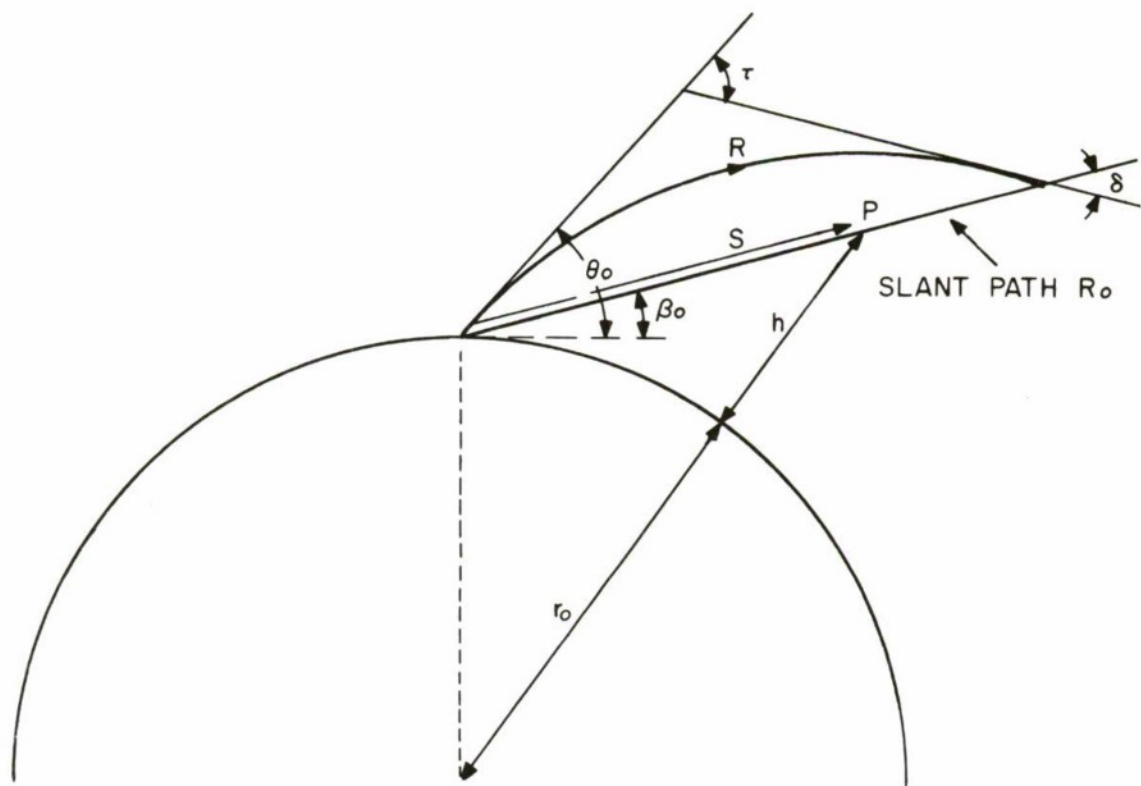


FIGURE 1 RAY GEOMETRY

Under the condition that

$$x^2 \gg 2 \quad (5)$$

$$\text{then } \exp(x^2) \int_x^\infty \exp(-t^2) dt \simeq 1/2 x \quad (6)$$

and since

$$\text{erf } x = 1 - \frac{2}{(\pi)^{\frac{1}{2}}} \int_x^\infty \exp(-t^2) dt \quad (7)$$

substituting for the error function in Equations (2) and (3) and making use of the Equations (6) and (7) gives

$$\Delta R \simeq \frac{N_s}{10^6 c \sin \beta_0} \left[1 - \frac{g \exp[g^2]}{(k+g) \exp[(k+g)^2]} \right] \quad (8)$$

$$\tau \simeq - \frac{N_s}{10^6 \tan \beta_0} \left[1 - \frac{g \exp[g^2]}{(k+g) \exp[(k+g)^2]} \right] \quad (9)$$

where, from (2)

$$k = R \left(\frac{c}{2 r_0} \right)^{\frac{1}{2}} \cos \beta_0 \quad (10)$$

$$\text{and } g = \left(\frac{c r_0}{2} \right)^{\frac{1}{2}} \tan \beta_0 \gg (2)^{\frac{1}{2}} \quad (11)$$

$$\text{and } (k+g) = R \left(\frac{c}{2 r_0} \right)^{\frac{1}{2}} \cos \beta_0 + \left(\frac{c r_0}{2} \right)^{\frac{1}{2}} \tan \beta_0 \gg (2)^{\frac{1}{2}} \quad (12)$$

As the range becomes very large, k increases and Equations (8) and (9) reduce to

$$\Delta R = \frac{N_s}{10^6 c \sin \beta_0} \quad (13)$$

$$\tau = \frac{N_s}{10^6 \tan \beta_0} \quad (14)$$

For $\theta_0 > 200$ mr, then β_0 may be replaced by θ_0 without serious error, and Equations (13) and (14) then take on a familiar form for high angle tracking. ⁷

3. A CORRECTION AT SMALL ELEVATION ANGLES

It was noted⁵ that the original Equations (2) and (3) give larger values of the range error and path bending than is actually true because the slant path, R_0 , lies below the ray path, R . Since the magnitude of refractivity is larger along R_0 than at the higher level along R , this result is not unexpected. Replacing β_0 by the apparent elevation angle, θ_0 , generates a path which will lie above the true propagation path therefore giving values which are too small. These differences become most noticeable, of course, at small elevation angles.

As the true elevation angle, β_0 , becomes smaller the conditions on the substitution for the error function becomes invalidated (reference Equation (11)). In fact, it is found that even if β_0 is replaced by θ_0 , the calculated values from Equations (8) and (9) will always be too large, particularly at small elevation angles.

In order to maintain the usefulness of the exponential functions at small angles a substitution for $\sin \beta_0$ was selected to be

$$\sin \beta_0 = \sin \gamma' = \sin \theta_0 + k_0 (\exp [-k_1 \theta_0^2]) \quad (15)$$

The constant, k_1 , is selected to make β_0 approach θ_0 at higher elevation angles which has physical meaning. Secondly, in the region of zero elevation angles the Equations (8) and (9) remain finite and can be constrained to provide meaningful results by the suitable selection of k_0 . Comparisons with ray-tracing data, as will be shown, indicate this form is acceptable and is convenient to use in calculations.

Equation (8), for example, then becomes

$$\Delta R \simeq \frac{N_s}{10^6 c \sin \lambda'} \left[1 - \frac{g \exp [g^2]}{(k + g) \exp [(k + g)^2]} \right] \quad (16)$$

where g and k are defined as

$$g = \left(\frac{c}{2} \frac{r_0}{r_0} \right)^{\frac{1}{2}} \tan \gamma' \quad (17)$$

$$k = R \left(\frac{c}{2} \frac{r_0}{r_0} \right)^{\frac{1}{2}} \cos \gamma' \quad (18)$$

and the angle γ' is derived from Equation (15) using selected constants R_0 , k_1 and the apparent elevation tracking angle, θ_0 .

At long ranges and zero elevation angle, Equation (16) reduces to

$$\Delta R = \frac{N_s}{10^8 c k_0} \quad (19)$$

Using available ray-tracing data for the CRPL exponential model atmosphere¹ for R greater than 2600 km, and with

$$N_s = 344.5$$

$$c = 0.157$$

then the range error is listed to be 0.1164 km.

Substituting in Equation (19) gives

$$k_0 = 0.0189$$

Also for $\theta_0 > 200$ mr it was desired that

$$\sin \gamma' \rightarrow \sin \theta_0.$$

Again comparing with ray-tracing data the constant k_1 was selected to be 200; therefore,

$$\sin \gamma' = \sin \theta_0 + 0.0189 \exp [-200 \theta_0^2]. \quad (20)$$

Figure 2 shows a comparison of calculations using Equations (16), (17), (18), and (20) with available ray-tracing data.

A range of 600 km was selected for the comparison in order not to eliminate the exponential terms in Equation (16).

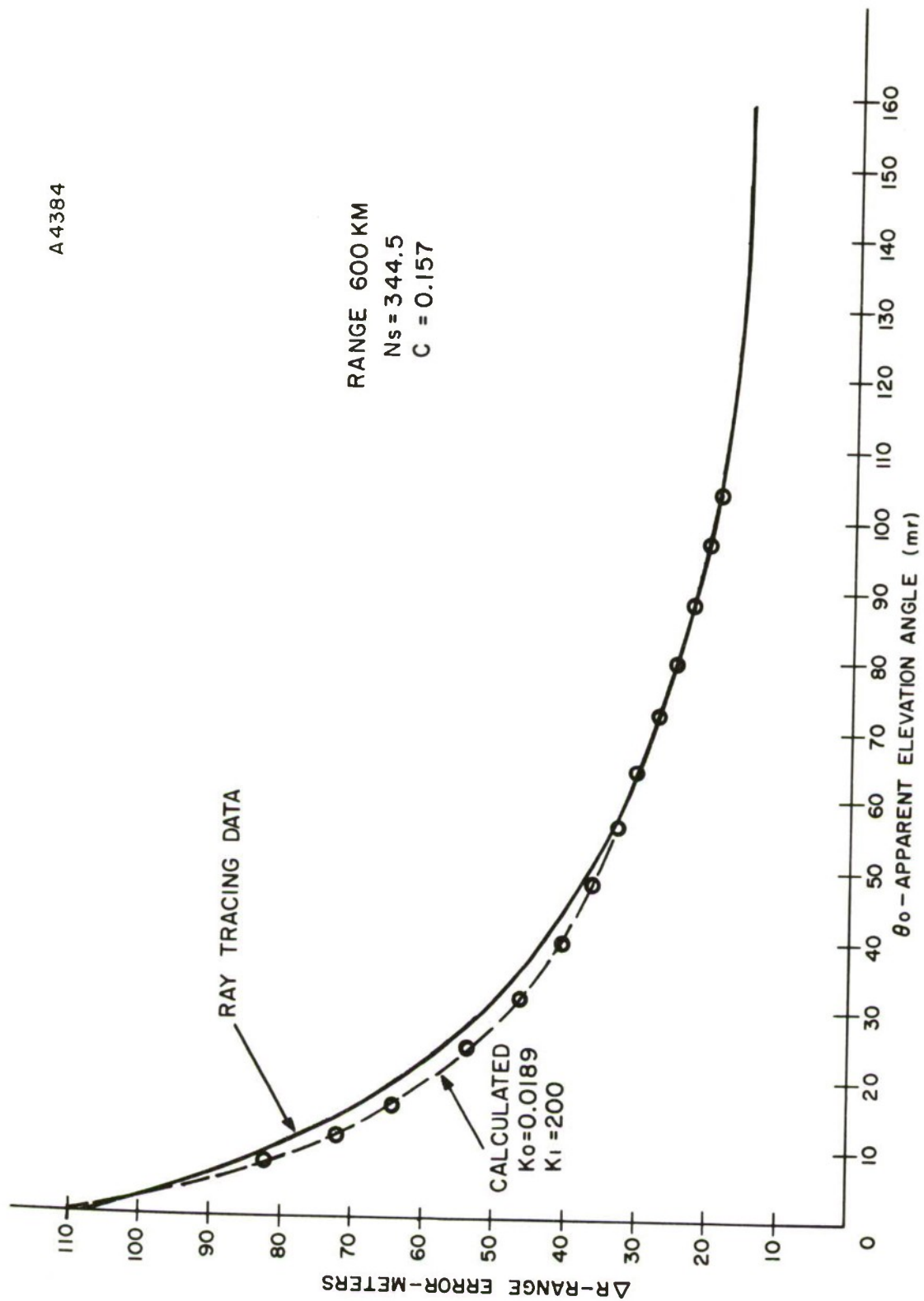


FIGURE 2 RANGE ERROR VS. APPARENT ELEVATION ANGLE
- LONG RANGE CASE (600 KM)

4. THE EFFECT OF REDUCED RANGES

As the range decreases the exponential ratio in brackets, Equations (8) and (9), approaches unity and causes the range error and path bending magnitudes to decrease, which is meaningful. However, at very small elevation angles, the quantity g becomes small as shown by Equation (11). Now as the range, R , decreases the condition on $(k + g)$, Equation (12), becomes invalidated. This combination of small angles and reduced ranges again sets a condition which reduces the accuracy of the calculations.

In the same way as $\sin \beta_0$ was modified to maintain accuracy at small angles a further modification was used to constrain the range dependent effect, again at small angles.

A convenient and useful form was to replace γ' by a new angle where

$$\sin \gamma = \sin \theta_0 + [k_0 + k_2 \exp(-k_3 R^2)] \exp(-k_1 \theta_0^2). \quad (21)$$

$\sin \gamma$ then approaches the original form, Equation (15), as the range becomes large and approaches $\sin \theta_0$ under all conditions as the elevation angle becomes large. At some minimum elevation angle, for example, 10 mr, $\sin \gamma$ is set equal to a function of k_2 , k_3 , and range. Using two extreme range situations, such as R equals 50 km and 600 km, tabulated ray-tracing data will provide values for the range errors from which k_2 and k_3 may be determined.

The simplest approach is to assume that $\exp(-k_3 R^2)$ is unity at ranges under 100 km and k_2 is then directly determined to provide agreement between the ray-tracing data and the new form of Equation (16), where $\sin \gamma$ is now defined by Equation (21). The further requirement, having selected k_2 is that the factor

$$k_2 \exp(-k_3 R^2) \ll k_0 \quad (22)$$

for $R_0 > 600$ km.

This latter requirement does not impose any difficulty on a suitable selection for k_3 once k_2 is determined.

Although the modification to the initial equations has centered around discussion of the range errors, the bending equation is affected by all the same considerations; therefore, the final form of Equations (8) and (9) becomes:

$$\Delta R \simeq \frac{N_s}{10^6 c \sin \gamma} \left[1 - \frac{g \exp [g^2]}{(k + g) \exp [(k + g)^2]} \right] \quad (23)$$

$$\tau \simeq - \frac{N_s}{10^6 \tan \gamma} \left[1 - \frac{g \exp [g^2]}{(k + g) \exp [(k + g)^2]} \right] \quad (24)$$

$$\sin \gamma = \sin \theta_0 + [k_0 + k_2 \exp (-k_3 R^2)] \exp(-k_1 \theta_0^2) \quad (25)$$

$$g = \left(\frac{c r_0}{2} \right)^{\frac{1}{2}} \tan \gamma \quad (26)$$

$$k = R \left(\frac{c}{2 r_0} \right)^{\frac{1}{2}} \cos \gamma \quad (27)$$

and the angle γ is derived from Equation (25).

Figures 3 and 4 show a comparison of calculated values of range error, ΔR , and path bending, τ , respectively, with the CRPL tabulated ray-tracing data. The constants in the $\sin \gamma$ function were selected to provide reasonable agreement over a wide range of possible radar tracking conditions. Certainly in practice for a particular region of angles and ranges of interest the selection of the four constants could be optimized.

A least squares smoothing program will be available shortly to allow a rapid calculation of all constants to give the best overall agreement with tabulated ray-tracing data.

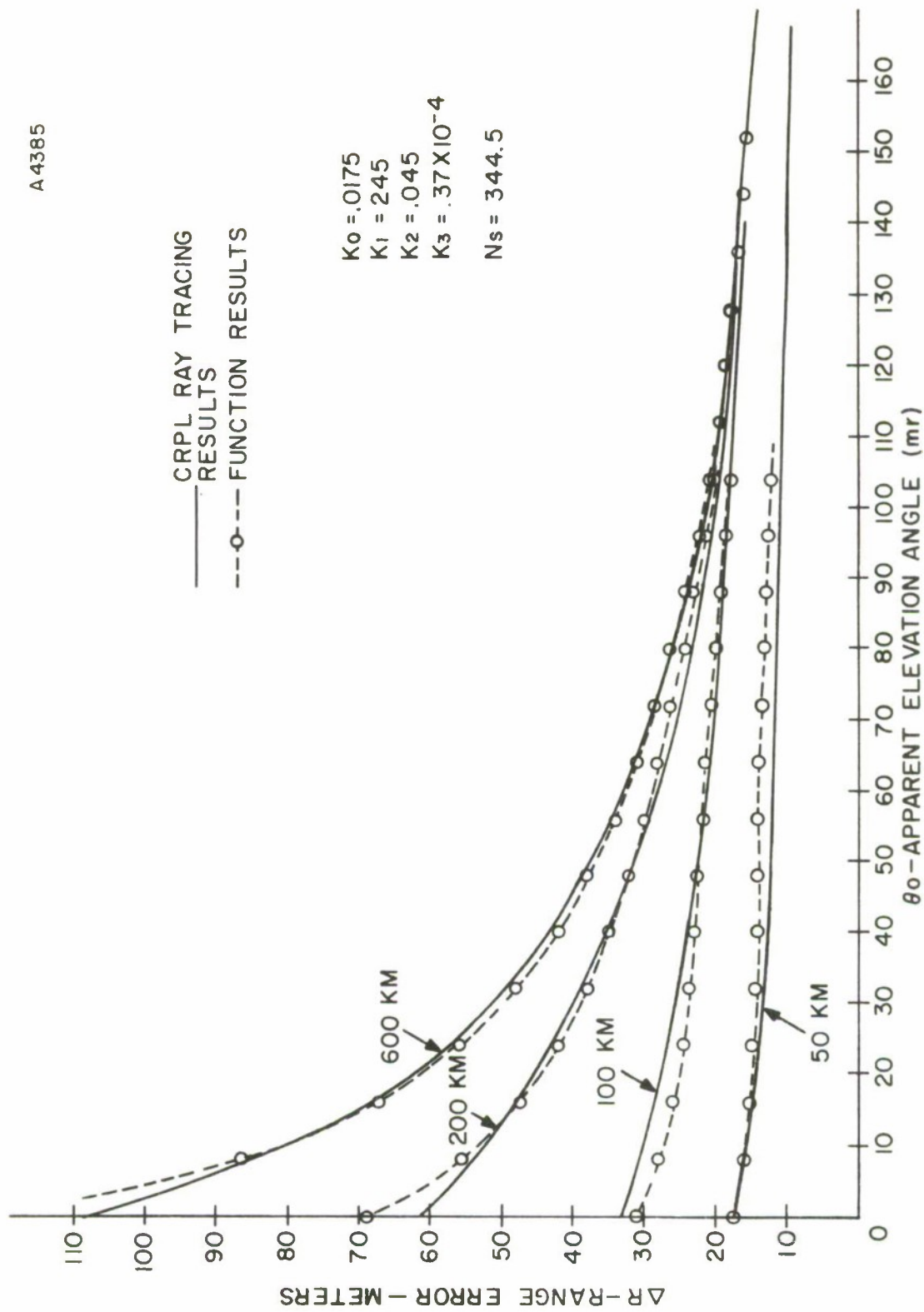


FIGURE 3 RANGE ERROR VS. APPARENT ELEVATION ANGLE
- VARIABLE RANGE CASE

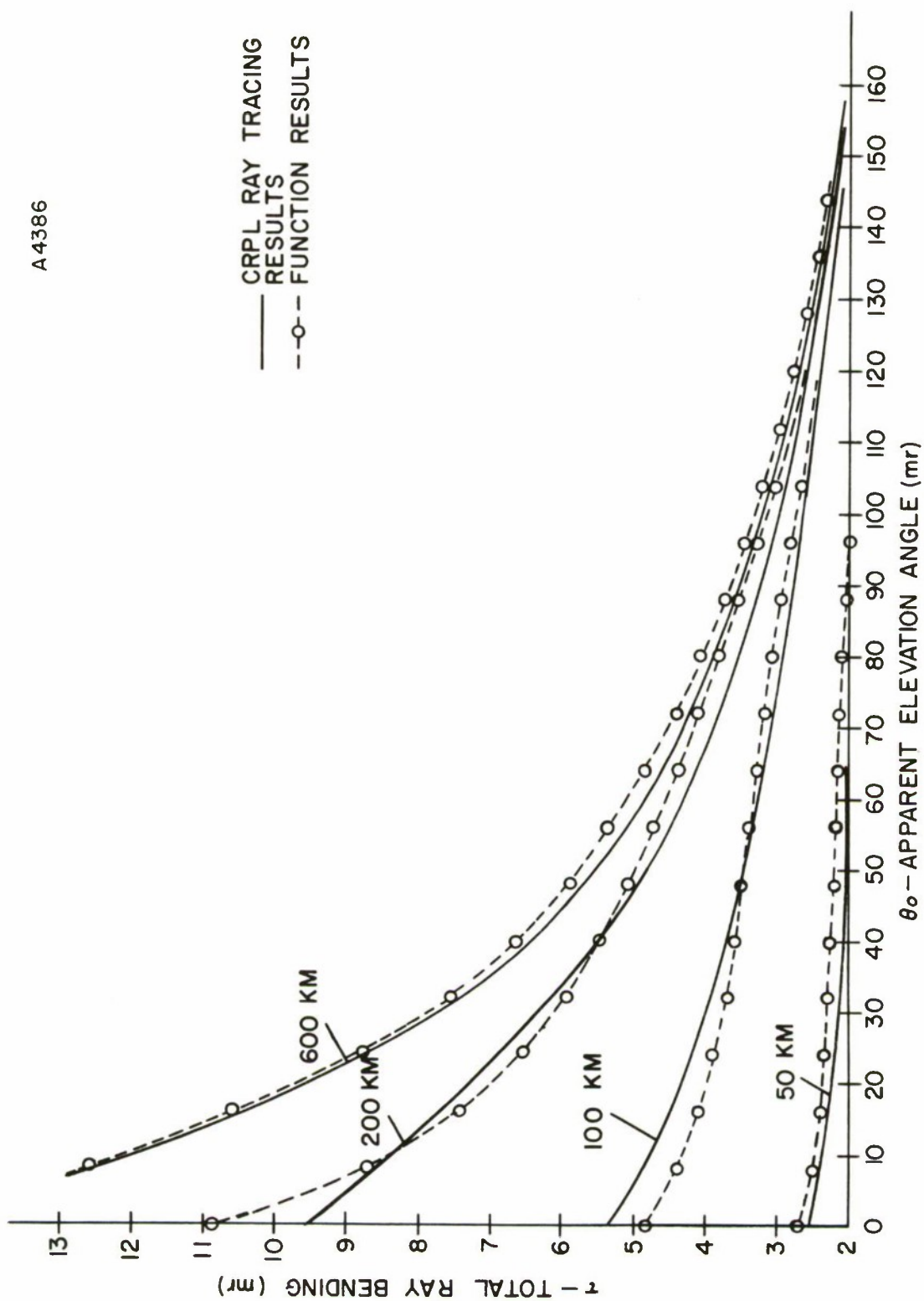


FIGURE 4 TOTAL PATH BENDING VS. APPARENT ELEVATION ANGLE
- VARIABLE RANGE CASE

5. THE SENSITIVITY OF CALCULATED MAGNITUDES WITH RESPECT TO CHANGES IN THE EXPONENTIAL MODEL PROFILE

The previous selection of constants was related to a CRPL model with a surface value of 344.5 N units. As the surface value changes, the decay constant, c , is correspondingly changed in accordance with the equation developed for this CRPL model.

A severe perturbation was introduced in the calculations by choosing a station value of N_s equal to 200 N units and with a corresponding decay constant of 0.118. Figures 5 and 6 show calculations of the range error, ΔR , and the overall path bending, τ , again compared against CRPL ray-tracing data for the above particular profile and for an intermediate and long range case.

The difference between the sets of curves has increased most significantly under two degrees (35 mr) elevation angle. The original refractivity profile, with a station value of 344.5 represents very moist conditions whereas the station condition of 200 represents dry conditions well above sea level. This station value could represent tracking from an airborne platform.

The significant conclusion is that the equations can be used to represent a wide range of possible tracking situations and environments. In practice one would select the constants to provide good agreement for the average local environmental conditions and the equations could then effectively absorb variations above the average without one having to regenerate a new set of constants.

The CRPL model was used in the previous comparisons because the ray-tracing data were available in a convenient form. Of course, these equations can be adapted to any other exponential model providing a set of accurate ray-tracing data are available to determine the constants.

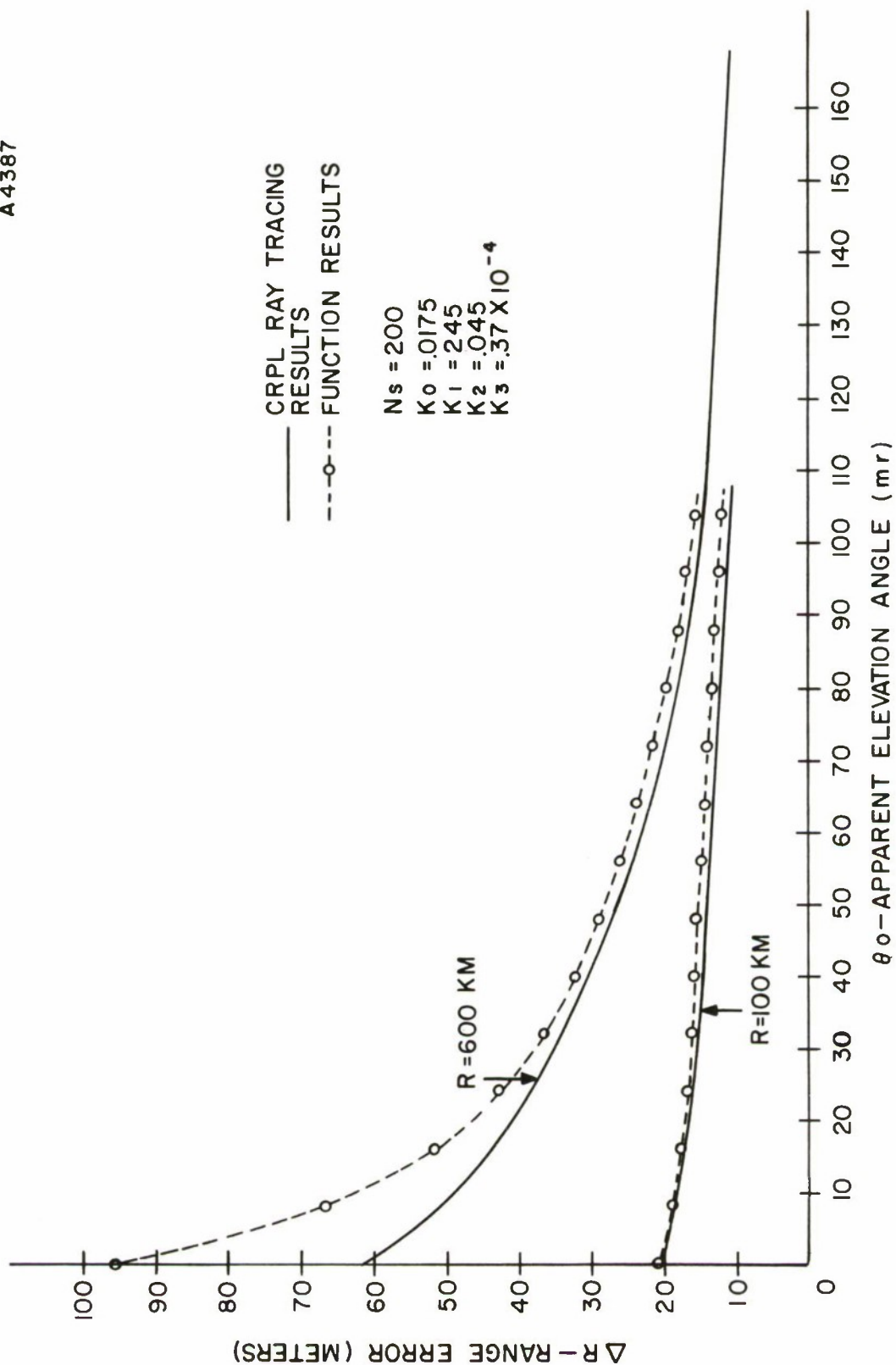


FIGURE 5 RANGE ERROR VS. APPARENT ELEVATION ANGLE
- EFFECT OF LARGE CHANGE IN REFRACTIVITY PROFILE

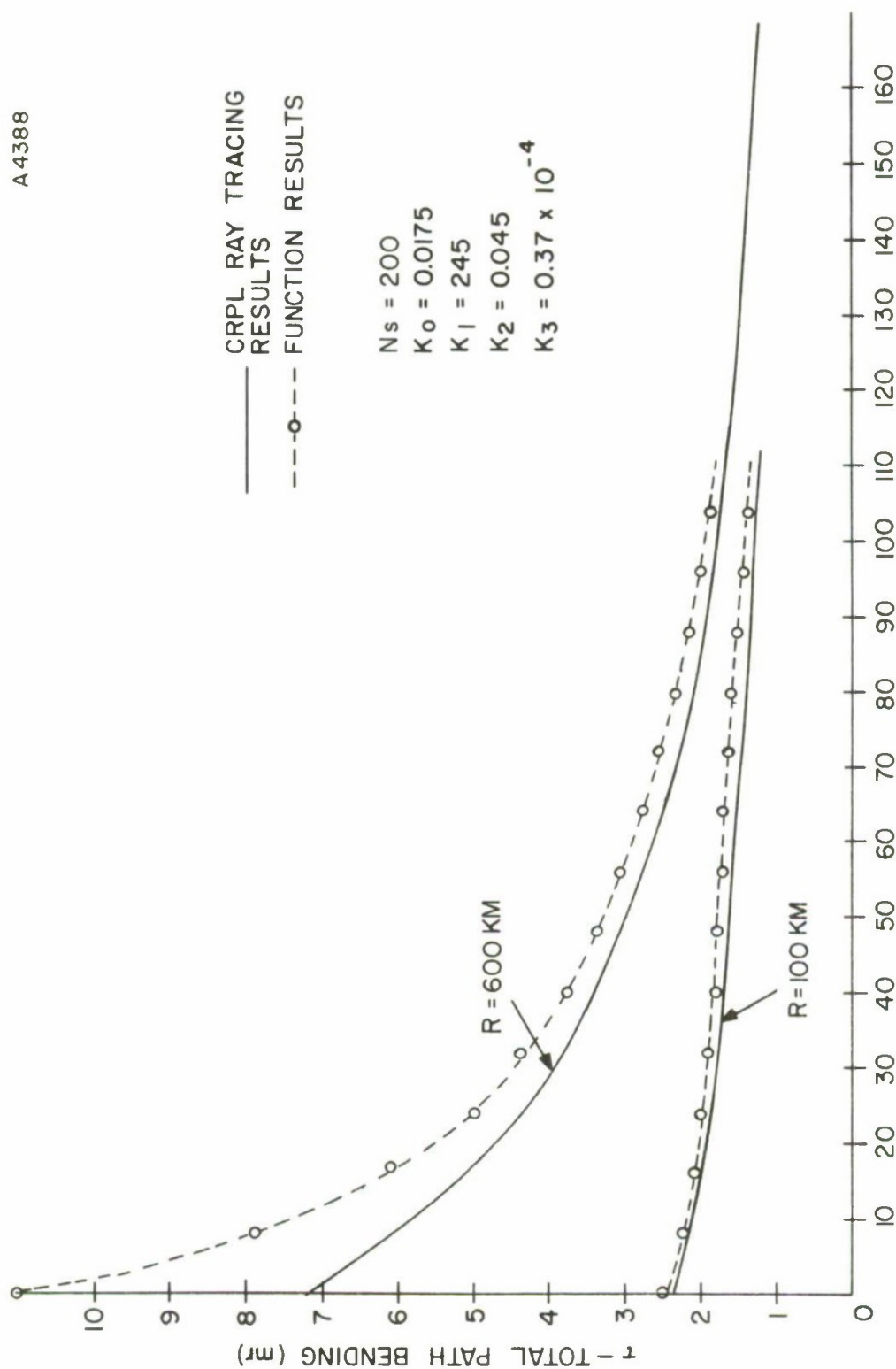


FIGURE 6 TOTAL PATH BENDING VS. APPARENT ELEVATION ANGLE
 - EFFECT OF LARGE CHANGE IN REFRACTIVITY PROFILE

6. A METHOD TO DETERMINE THE ELEVATION ANGLE ERROR

In general, the ray-path bending calculations have little application because only at extremely long ranges, in fact, when the target is outside the real atmosphere, does the overall bending, τ , approach the value for the elevation angle error, ϵ . The elevation angle error is very important information in most tracking situations, particularly where position information is required with only a knowledge of apparent range and elevation angle.

From Figure 7 the angle, θ_1 , is given by

$$\theta_1 = \tau + \left(\frac{\pi}{2} - \theta_0 \right) \quad (28)$$

Also, the slope of the ray at any point, P (x, y) is

$$\frac{dy}{dx} = \tan \left(\frac{\pi}{2} - \theta_1 \right) \quad (29)$$

$$\text{and} \quad \sin \theta_1 = \frac{dx}{dR} \quad (30)$$

Substituting (28) and (30) into (29) gives

$$y = \int_0^R \sin (\theta_0 - \tau) dR \quad (31)$$

As mentioned previously, the geometric difference in length between the measured ray-path range and the slant range is small. From Equation (31) the true elevation angle, β_0 , can then be approximated by

$$\sin \beta_0 \simeq \frac{1}{R} \int_0^R \sin (\theta_0 - \tau) dR \quad (32)$$

Therefore, the elevation angle error, ϵ , is

$$\epsilon \simeq \theta_0 - \sin^{-1} \left[\frac{1}{R} \int_0^R \sin (\theta_0 - \tau) dR \right] \quad (33)$$

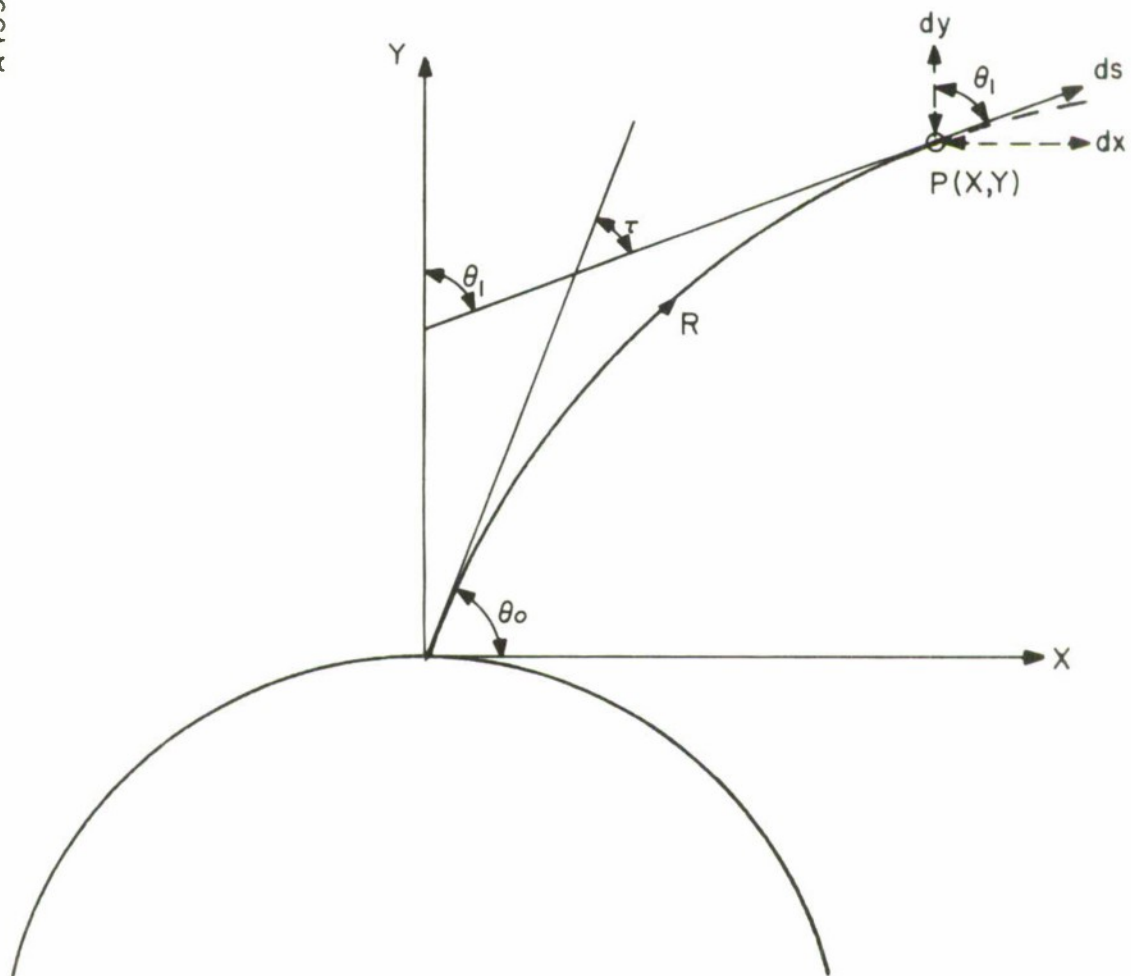


FIGURE 7 RAY GEOMETRY USED TO CALCULATE THE ELEVATION ANGLE ERROR

Replacing τ from Equation (24) leads to a solution since the integral is then a function of R . However, the term $\tan \gamma$ in the denominator of (24) complicates the integral and at this time a solution has not been found. The second approach was to remove $\tan \gamma$ from the integral by considering its mean value over R . This approach led to significant errors at small elevation angles.

The most satisfactory solution was to evaluate the integral directly by the summation of terms, where

$$\int_0^R \sin(\theta_0 - \tau) dR \simeq \sum_{i=1}^n \sin(\theta_0 - |\tau|_i) \cdot (\delta R_i) \quad (34)$$

where τ_i is the value in the i^{th} interval

and δR_i is the i^{th} interval.

Figures 8 and 9 show a comparison of results for two ranges of 600 and 200 km, respectively, and with the integral approximated by ten terms in the summation. The difference between results is most noticeable at the short ranges. However, referring to the bending calculations, Figure 4, it is seen that the τ values are not in exact agreement with the ray-tracing data; therefore, one would not expect the ϵ values to be any better.

Since the values for $|\tau|_i$ are not linearly dependent upon range consideration should be given to a weighting factor which would increase the number of terms in the sum at shorter ranges. This approach is being considered in the optimization analysis and results will be presented at a later date.

At long ranges, τ becomes essentially independent of range and the integration of Equation (33) gives

$$\epsilon = \theta_0 - \sin^{-1} [\sin(\theta_0 - |\tau|)] \quad (35)$$

In this case, Equation (35) gives

$$\epsilon = |\tau| \quad (36)$$

As ray tracing data shows¹² this approximation is only useful where tracking ranges in excess of 3000 km are involved.

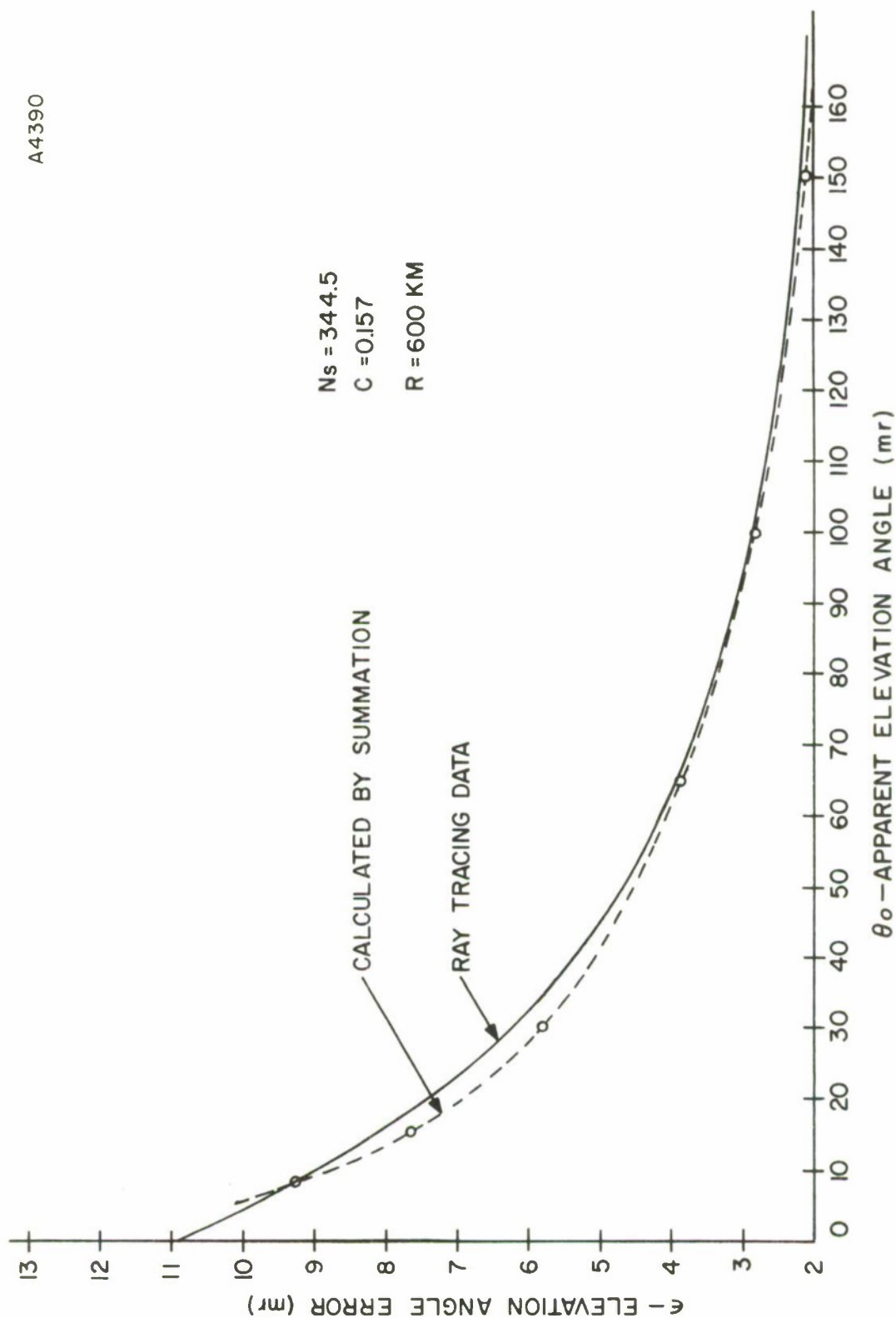


FIGURE 8 ELEVATION ANGLE ERROR VS. APPARENT ELEVATION ANGLE
 - LONG RANGE CASE (600 KM)

A4391

$N_s = 344.5$
 $C = 0.157$

$R = 200 \text{ KM}$

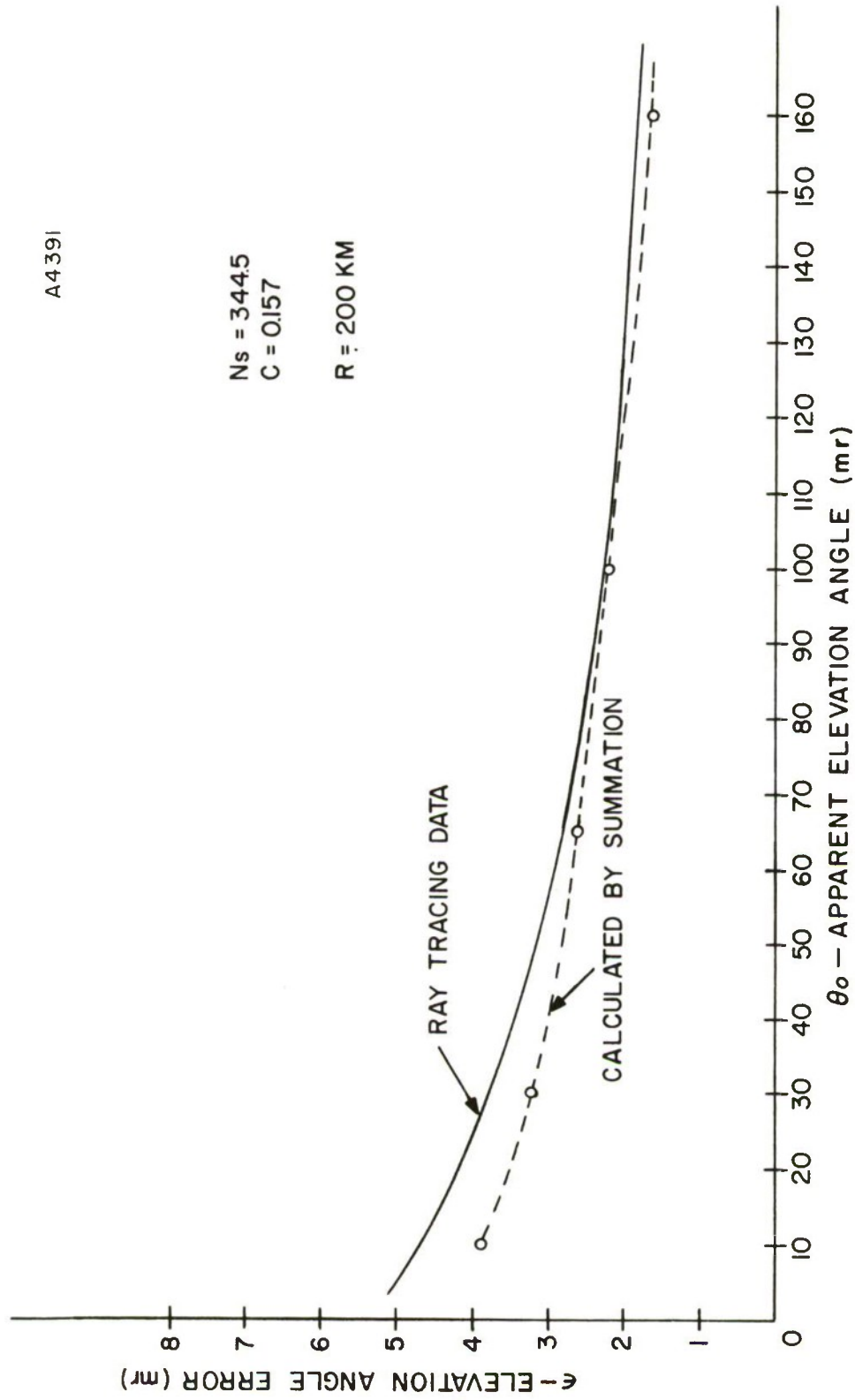


FIGURE 9 ELEVATION ANGLE ERROR VS. APPARENT ELEVATION ANGLE
 - MEDIUM RANGE CASE (200 KM)

7. AN APPROXIMATE SOLUTION FOR THE DOPPLER VELOCITY ERROR ANGLE

Referring to Figure 10, the doppler velocity error in the radial direction attributed to refraction can be shown to be⁸

$$\Delta V \simeq V \sin \psi(\delta) \quad (37)$$

where V is the actual target velocity

ψ is the angle between the velocity vector and the direct slant path, R_0 ,

and δ is the local angle between the ray direction and the slant path.

From the measurements of the range, apparent elevation angle, and, therefore, the calculated elevation angle error (Equation (33)), it is possible to determine the apparent target velocity and its direction of motion. Then the calculation of the angle, δ , will provide a first order correction to the velocity measurement error produced by the ray path bending.

From Equation (32), $\sin \beta_0$ is

$$\sin \beta_0 \simeq \frac{1}{R} \int_0^R \sin(\theta_0 - \tau) dR \quad (38)$$

Expanding $\sin(\theta_0 - \tau)$ and assuming τ to be a small quantity, which is generally true, then

$$\sin(\theta_0 - \tau) \simeq \sin \theta_0 - \tau \cos \theta_0 \quad (39)$$

Substituting (39) in (38) and substituting for the magnitude of τ from (24) gives

$$\begin{aligned} \sin \beta_0 \simeq \sin \theta_0 - \frac{N_s \cos \theta_0}{10^6 R} \int_0^R \frac{dR}{\tan \gamma} \\ + \frac{N_s \cos \theta_0}{10^6 R} \int_0^R \frac{g \exp[g^2]}{\tan \gamma (g+k) \exp[(g+k)^2]} dR \end{aligned} \quad (40)$$

For long ranges γ is essentially independent of range, according to the method of selecting the constants given by Equation (22). Then for small elevation angles, Equation (40) can be written

$$\beta_0 \simeq \theta_0 - \frac{N_s \cos \theta_0}{10^6 \tan \gamma} + \frac{N_s \cos \theta_0}{10^6 R \tan \gamma} \int_0^R \frac{g \exp[g^2]}{(k+g) \exp[(k+g)^2]} dR \quad (41)$$

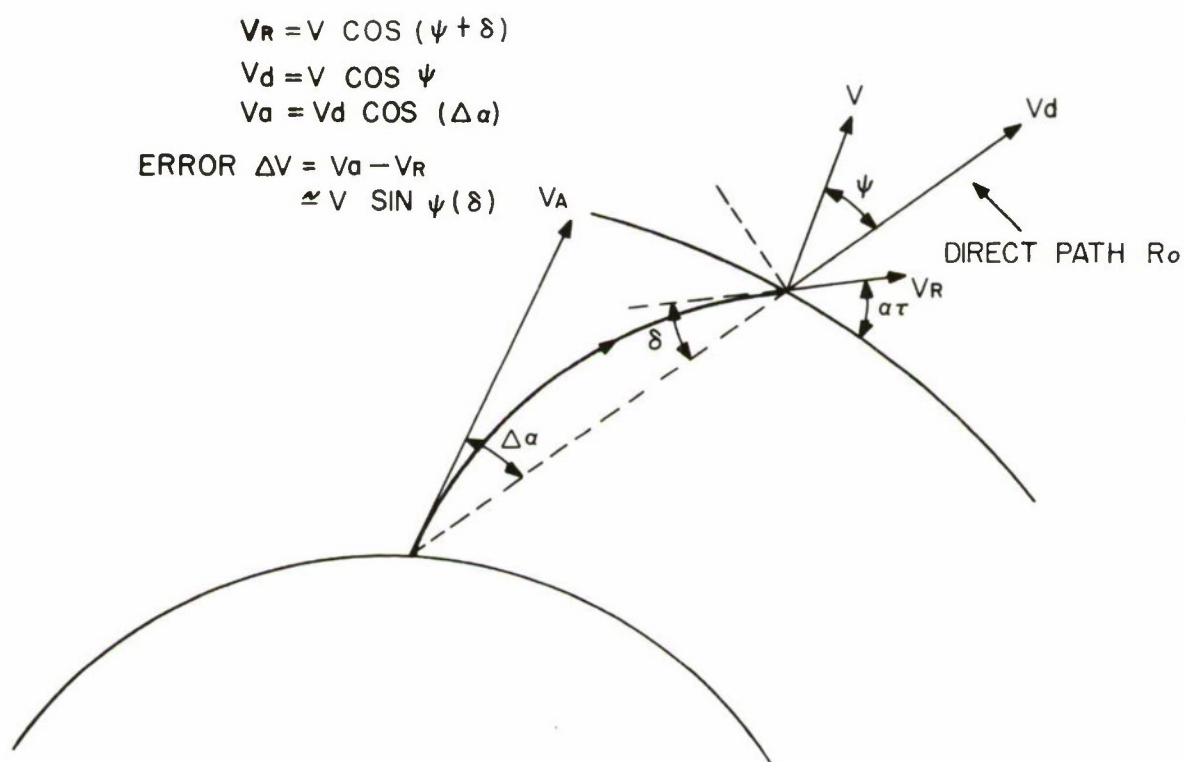


FIGURE 10 DOPPLER ERROR ANGLE GEOMETRY

From the definition of g and k , Equations (26) and (27), the last term in Equation (41) can be written

$$\int_0^R \frac{g \exp [g^2] dR}{(k+g) \exp [(k+g)^2]} = g \int_0^R \frac{\exp [-(a^2 R^2 + 2 a g R)]}{(a R + g)} dR \quad (42)$$

where $a = \left(\frac{c}{2 r_0}\right)^{\frac{1}{2}} \cos \gamma$.

Completing the square in the exponent and setting

$$x = a R + g \quad (43)$$

then Equation (42) becomes

$$\int_0^R \frac{g \exp [g^2] dR}{(k+g) \exp [(k+g)^2]} = \frac{g \exp [g^2]}{a} \int_g^{(aR+g)} \frac{\exp [-x^2]}{x} dx \quad (44)$$

$$= \frac{g \exp [g^2]}{2a} \int_{g^2}^{(aR+g)^2} \frac{\exp (-t)}{t} dt \quad (45)$$

where $x^2 = t$

The integral of Equation (45) can be evaluated by expanding and integrating to give

$$\begin{aligned} \int_{g^2}^{(aR+g)^2} \frac{\exp (-t)}{t} dt &= \ln \left[\frac{k+g}{g} \right] + \sum_{n=1}^{\infty} \frac{(-1)^n (k+g)^{2n}}{n \cdot n!} \\ &\quad - \sum_{n=1}^{\infty} \frac{(-1)^n g^{2n}}{n \cdot n!} \end{aligned} \quad (46)$$

$$= E_i [g^2] - E_i [(k+g)^2] \quad (47)$$

where $E_i(z)$ is the exponential integral defined by

$$E_i(z) = \int_z^{\infty} \frac{\exp (-u)}{u} du$$

Then, from Equation (41), β_0 can be written

$$\beta_0 \simeq \theta_0 - \frac{N_s \cos \theta_0}{10^6 \tan \gamma} + \frac{N_s \cos \theta_0 g \exp [g^2]}{10^6 2 k \tan \gamma} [E_i [g^2] - E_i [(k+g)^2]] \quad (48)$$

where $k = a R$.

From Figure 1,

$$\begin{aligned}\beta_0 &= \theta_0 - \epsilon \\ &= \theta_0 - \tau + \delta\end{aligned}\tag{49}$$

A comparison of Equations (24), (48), and (49) suggests that at long ranges then τ can be identified with the second term in Equation (48) at small elevation angles. Also, from (48) and (49) the doppler velocity error angle, δ , can be identified with the last term in (48), and

$$\delta \simeq \frac{N_s \cos \theta_0 g \exp [g^2]}{10^6 2k \tan \gamma} [E_i [g^2] - E_i [(k + g)^2]]\tag{50}$$

Figure 11 shows a comparison of the calculated value of δ with ray-tracing data. A range of 600 km was chosen to ensure that γ would be independent of range.

The agreement is reasonable except at very small angles where, of course, the previous calculations for ϵ also deviated from the ray-tracing data.

The validity of the solution is again dependent upon having a range sufficiently large such that γ is range independent and that the elevation angles are sufficiently small to justify the expansion in Equations (39) and (41). Since the angle, δ , does not become significant in practice, except at lower elevation angle tracking, the latter condition does not impose any practical difficulty.

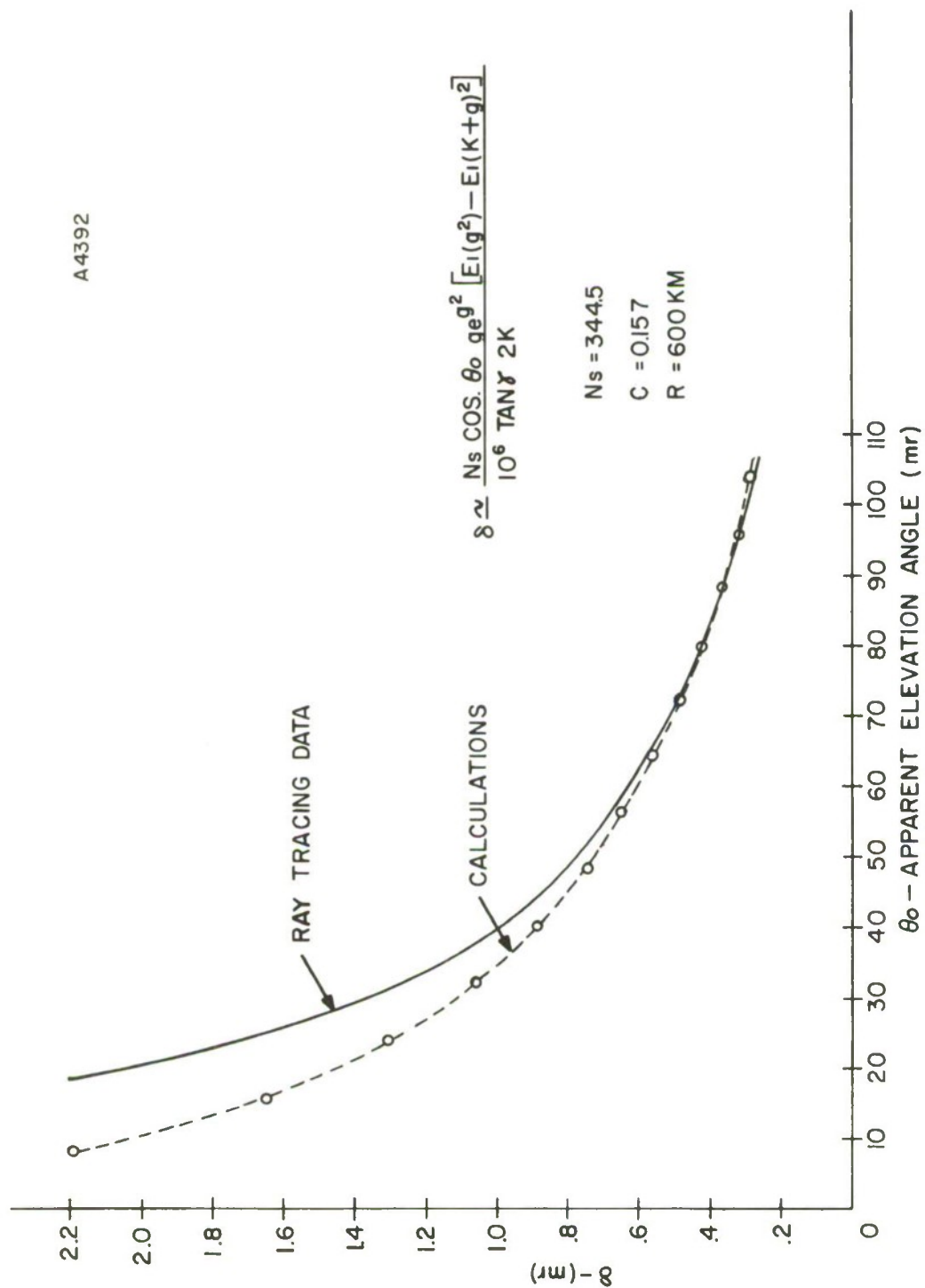


FIGURE 11 DOPPLER VELOCITY ERROR ANGLE VS. APPARENT ELEVATION ANGLE
- LONG RANGE CASE (600 KM)

8. SOME FINAL COMMENTS

It is evident in the development of the elevation angle error equation that the calculation of ϵ will be no better than the ray-path bending values for τ . In turn, the ϵ values directly influence the values obtained for δ , the doppler velocity error angle. In practice, therefore, if one is satisfied with using an exponential model to define the propagation conditions, every effort should be made to select the k constants to give good calculations for τ over the range of interest.

Referring to Equations (23) and (24), it is seen that the range error and the path bending are related by the equation

$$\tau = -c \cos \gamma (\Delta R). \quad (51)$$

For real-time tracking operations this simple relationship provides immediate values of path bending as the range errors are being calculated. In practice, this ability is significant.

The basic development of the equations has suggested other approaches and refinements which were not pursued in this paper. The attempt herein was to derive the simplest types of equations for use in real-time tracking applications at the expense of rigor and maximum possible accuracy. The development of a least squares smoothing program will provide a method to determine the constants k_0 through k_3 to give the best comparison with any particular set of ray-tracing data. Two ray-tracing programs presently available can be used to generate tabulated data for any exponential model atmosphere.

REFERENCES

1. Bean, B. R., and Thayer, G. D., "CRPL Exponential Reference Atmosphere," NBS Monograph 4, (October 29, 1959).
2. Bean, B. R., and Thayer, G. D., "On Models of the Atmospheric Refractive Index," Proc IRE 47, No. 5, 740-755, (May 1959).
3. Thayer, G. D., "A Formula for Radio Ray Refraction in an Exponential Atmosphere," Journal of Research, NBS, D. Radio Propagation, Vol. 65, No. 2, March-April 1961.
4. Freeman, J. J., "Range Error Compensation for a Troposphere With Exponentially Varying Refractivity," NBS, J. Res. 66 D No. 6, November-December 1966.
5. Freeman, J. J., "The Real-Time Compensation for Tropospheric Effects on the Measurement of Range and Range Rate," Proc. of the Second Tropospheric Refraction Effects Technical Review Meeting, Electronics Systems Division of Air Force Systems Command, Bedford, Massachusetts, ESD-TR-64-103, Vol. II, April 1964.
6. Abramowitz, M., and Stegun, J. A., "Handbook of Mathematical Functions", NBS Applied Mathematics Series 55, June 1964.
7. Bean, B. R., and Dutton, E. J., "Radio Meteorology," NBS Monograph 92, March 1966.
8. Millman, G. N., "Atmospheric and Extra Terrestrial Effects on Radio Wave Propagation," General Electric Company, Syracuse, New York, Report R61EMH29, June 1961.

UNCLASSIFIED
Security Classification

DOCUMENT CONTROL DATA - R & D

(Security classification of title, body of abstract and indexing annotation must be entered when the overall report is classified)

1. ORIGINATING ACTIVITY (Corporate author) Syracuse University Research Corporation Applied Sciences Division, Systems Synthesis Laboratory Merrill Lane, University Heights, Syracuse, New York		2a. REPORT SECURITY CLASSIFICATION UNCLASSIFIED	
		2b. GROUP N/A	
3. REPORT TITLE SIMPLE ANALYTICAL FUNCTIONS WHICH PROVIDE MAGNITUDES OF RANGE AND ANGLE ERRORS FOR PROPAGATION IN AN EXPONENTIAL ATMOSPHERE			
4. DESCRIPTIVE NOTES (Type of report and inclusive dates) None			
5. AUTHOR(S) (First name, middle initial, last name) Lyll G. Rowlandson			
6. REPORT DATE 19 January 1968		7a. TOTAL NO. OF PAGES	7b. NO. OF REFS
8a. CONTRACT OR GRANT NO. F19628-68-C-0209		9a. ORIGINATOR'S REPORT NUMBER(S) ESD-TR-68-308	
b. PROJECT NO.			
c.		9b. OTHER REPORT NO(S) (Any other numbers that may be assigned this report)	
d.			
10. DISTRIBUTION STATEMENT This document has been approved for public release and sale; its distribution is unlimited.			
11. SUPPLEMENTARY NOTES		12. SPONSORING MILITARY ACTIVITY Aerospace Instrumentation Program Office, Electronic Systems Division, AFSC, USAF, L G Hanscom Field, Bedford, Mass. 01730	
13. ABSTRACT The calculation of range and angle errors has been attempted by integrating the ray equations along the slant path and assuming an exponentially decreasing index of refraction with height. These equations are represented by error functions which are not simple analytical solutions. There is a further difficulty in relating the true elevation angle to the apparent elevation angle. The following paper shows how these equations may be modified to provide simple analytical functions. In the process the functions permit a range and apparent elevation angle term to be included which not only correct for the approximate solution at small angles but also generate functions which remain continuous through zero elevation angle. A comparison with ray-tracing calcu- lations demonstrates that these functions can be used to compute meaningful magnitudes of range, elevation angle and doppler velocity errors.			

14. KEY WORDS	LINK A		LINK B		LINK C	
	ROLE	WT	ROLE	WT	ROLE	WT
Refraction Radar Tracking Corrections Propagation Exponential Atmosphere						